Acceptance criteria for accelerated aging testing of silvered-glass mirrors for Concentrated Solar Power Technologies

Florian Sutter [a,*], Aránzazu Fernández-García[b], Johannes Wette [a], Tomás Jesús Reche-Navarro [a], Lucía Martínez-Arcos [b]

[a] DLR German Aerospace Center, Institute of Solar Research, Plataforma Solar de Almeria, Ctra. Senés Km. 4, P.O.Box 44, 04200, Tabernas, Almería (Spain),
[b] CIEMAT, Plataforma Solar de Almeria, Ctra. Senés Km. 4, P.O. Box 22, 04200, Tabernas, Almería (Spain),

* Corresponding author: Tel.: +34 950 277 684, Fax.: +34 950 260 315; E-mail address: Florian.Sutter@dlr.de

Abstract

Solar reflectors for Concentrating Solar Power (CSP) technologies are required to maintain their optical properties in demanding environments for more than 20 years of service-life. The durability of the commonly used silvered-glass reflectors is typically qualified by means of accelerated aging. Recently, the Spanish standardization committee UNE has published the first specific standard for this topic, which defines a set of accelerated aging tests for CSP reflectors. However, the standard does not contain pass/fail criteria. This paper proposes useful acceptance criteria for the accelerated tests defined by UNE, helping to interpret the obtained degradation results. The criteria have been determined by analyzing the collected accelerated aging data over the past 5 years in the OPAC laboratory, a joint research group of DLR and CIEMAT. Data from six different 4 mm silvered-glass manufacturers is presented, covering nearly the entire market of commercially available silvered-glass mirrors, and going way beyond the recommended testing times of the UNE standard. The data may be used to benchmark initial reflective properties (before aging) and the performance during accelerated durability testing. In addition, recommendations for improvements of the standard are given and an estimate of the acceleration factor of the Copper Accelerate Salt Spray (CASS) test with respect to a highly corrosive outdoor environment is presented.

Keywords: accelerated aging testing; solar reflector; reflectance; durability; acceptance criteria; concentrated solar power

1. Introduction

Silvered-glass reflectors have been the material of choice for CSP technologies since the very beginning; in fact they were used as reflective material for the SEGS plants erected in 1983. The used monolithic glass mirrors are typically comprised of a 4 mm

low-iron glass, although lower glass thicknesses are available. The reflecting silver layer is applied by wet chemical processes and protected by a copper layer, which retards the tarnishing of the silver. The metallic layers have a thickness of around 110-120 nm (see scanning electron microscope (SEM) image in Figure 1a). The copper layer is typically protected by three paint layers, often polyurethane based, and with a thickness of around 30 µm each (see Figure 1b). The function on the Titanium-based top coat is UV-protection and abrasion prevention. The intermediate coat acts as primer and diffusion barrier, while the base coat provides corrosion protection.

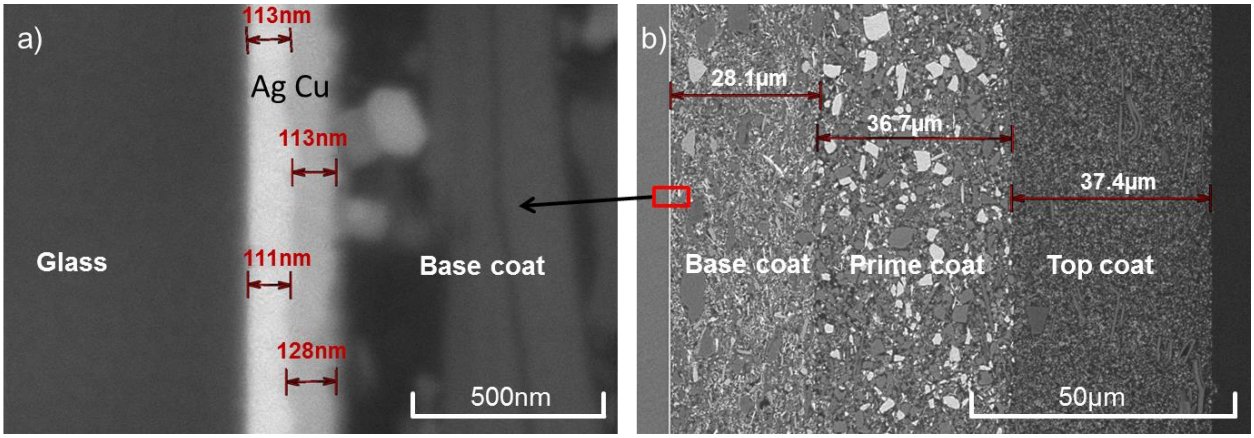

Figure 1 Typical glass mirror architecture viewed in SEM. a) Silver and copper layers. b) Protective back coatings.

The fact that after more than 30 years in SEGS plant operation most of the facets are still in service proofs their excellent durability. The corrosion and abrasion resistance of glass mirrors goes well beyond the durability of alternative mirrors on aluminum or polymer basis. Typical annual degradation rates in reflectance have reported to be about 0.002 for glass mirrors compared to ~0.008 for aluminum mirrors [1], [2].

However, the protective paint composition used in the early days of the SEGS plants with 10-20%-wt lead (Pb)-content changed throughout the years towards low-Pb content due to environmental concerns, with typical Pb- contents of 1%-wt [3]. The new low-Pb or even Pb-free paint layers paired with aggressive environmental conditions might become an issue for the lifetime of the glass mirrors. Figure 2 shows the common failure modes of silvered-glass mirrors during operation. Localized corrosion spots and edge corrosion are generally prone to humid and especially coastal sites. The impact of the corrosion on the reflectance loss of the mirror is usually marginal: the annually corroded area seldom exceeds 0.16% even in extremely aggressive exposure sites with industrial pollutants (see also section 3.7 and [5]). Typical annual corrosion areas are below 0.05% for desert areas. Tarnishing of the reflector surface may have a higher impact, accounting nearly entirely to the common reflectance loss of 0.002 reported in

[1]. Tarnishing may be caused by glass corrosion (which was only detected in specific areas of the CSP plants) and microscopic oxidation of the silver layer. Glass erosion may have strong impact on the losses caused by scattering. Annual losses in specular reflectance due to glass erosion of up to 0.004 and 0.027 have been reported for the Moroccan exposure sites Missour and Zagora respectively, where samples were exposed at 1.2 m height in desert environment without wind fence protection [4].

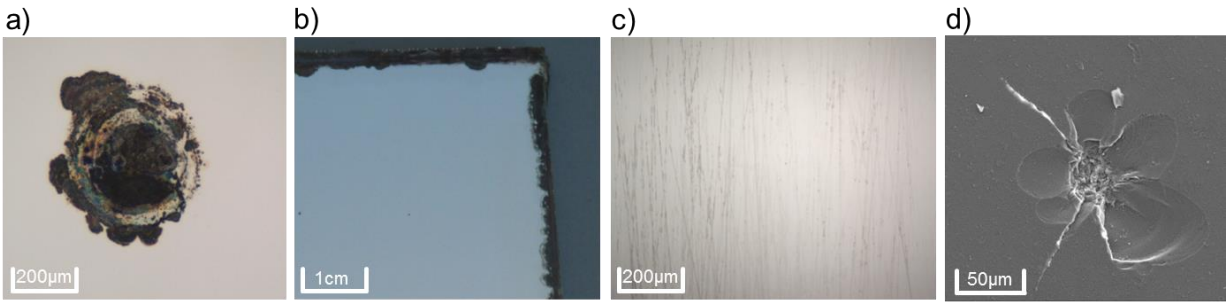

Figure 2 Common failure modes of silvered-glass reflectors during outdoor service. a) Localized corrosion spot in the silver layer after 12 months of exposure at the coastal site of Tan Tan, Morocco. b) Edge corrosion after 12 months of exposure at Tan Tan, Morocco. c) Tarnishing of reflector surface (of glass and silver layer) after 5 years of exposure in Southern Spain d) Erosion of glass after 26 months of exposure at desert site of Zagora, Morocco.

Accelerated aging testing uses intensified conditions of humidity, radiation, temperature, etc. and is typically used to qualify mirror durability [6], [7]. Deduction of a service life-time estimation based on these tests is a challenging task, requiring the accelerated test conditions to be as representative as possible for the outdoor conditions. On a different approach, material dependent constants may be derived by means of accelerated tests, which may then serve as input for life-time models [8]. Up to today, life-time estimations have only been developed for aluminum reflectors, based on outdoor degradation data up to 3 years in different environments [9], [10], [11], [12]. Despite no satisfying models for silvered-glass mirrors are available, accelerated aging is still a useful tool when it comes to compare the expected durability of different candidate materials, ranking material performance under defined climatic conditions. Also, it may be used as a quality control tool in running production, detecting possible problems in the coating lines.

The Spanish Association for Standardization, UNE (formerly AENOR), subcommittee AEN / CTN206 / SC117, has been working on standards of components for CSP plants since 2010 [13]. In 2018, UNE published a standard related to CSP mirrors, defining the accelerated aging tests summarized in Table 1 [14]. A more detailed description of the specific testing conditions can be found in [15] or the corresponding standards [16], [17],

[18]. The UNE standard only covers accelerated corrosion tests, simulating failure modes a-c in Figure 2. For accelerated erosion testing, a different procedure needs to be followed (e.g. as described in [19], [20]).

The UNE standard is the first one related truly to CSP mirrors. Former mirror testing was mainly based on component testing procedures for photovoltaic or concentrated photovoltaic technologies [21], [22]. However, the testing conditions defined in the UNE standard were not based on a scientific comparison of outdoor exposure experiments with accelerated aging data but according to some manufactures' experience. Recent research by Wette et al. [23] has shown that a silvered-glass mirror material, which corroded heavily during seven years of outdoor exposure in Abu Dhabi, exhibited almost no degradation during any of the UNE tests. Hence, correlation of the UNE standard to outdoor exposure seems questionable. In this paper, accelerated aging data is presented for nearly all current commercial mirror materials for testing times well beyond the recommended ones in UNE. Based on this data, pass/fail criteria are deduced, which will improve interpretation of the obtained test results of this standard and allow for benchmarking against the current state of the art.

Table 1: Overview of accelerated ageing tests of UNE 206016:2018 [14] standard (*T*= Temperature, *RH*= relative humidity)

Test	**Duration**	**Summary of testing conditions**
Neutral Salt Spray (NSS) ISO 9227	480 h	*T*=35±2 ºC, pH=[6.5, 7.2] at *T*=25±2 ºC Sprayed NaCl solution of 50 ± 5 g/l with condensation rate of 1.5 ± 0.5 ml/h on a surface of 80 cm²
Copper-accelerated acetic acid salt spray (CASS) ISO 9227	120 h	*T*=50±2 °C, pH=[3.1, 3.3] at *T*=25±2 ºC Sprayed NaCl solution of 50 ± 5 g/l and 0.26 ± 0.02 g/l of $CuCl_2$ Condensation rate of 1.5 ± 0.5 ml/h on a surface of 80 cm²
Condensation ISO 6270-2 CH	480 h	*T*=40±3 °C *RH*=100%, with condensation on the samples
Combined thermal cycling and humidity (TCH)	10 cycles (240 h)	4 h at *T*=85±2 °C, 4 h at *T*=-40±2 °C, Method A: 16 h at *T*=-40±2 °C and *RH*=97±3% Method B1: 16 h at *T*=85±2 °C and *RH*=85±3% Method B2: 40 h at *T*=65±2 °C and *RH*=85±3%
UV and humidity ISO 16474-3 (UVH)	2000 h	1 cycle: 4h at UV exposure at *T*=60±3 °C followed by 4h at *RH*=100% at *T*=50±3 °C

2. Materials and methods

Accelerated aging was performed on silvered-glass mirror specimens of 10x10 cm² size, usually cut out of full size facets directly coming from the production line. For the manufacturer of tempered glass, for which samples could not be cut, the tempering process was either omitted or small scale samples were coated separately, taking special care to reproduce the manufacturing conditions. Usually three samples were tested from each manufacturing batch. Each sample contained at least one originally sealed edge. Corrosion occurring at cut edges was not taken into account for analysis.

The CASS test was carried out in a salt spray chamber from the company Vötsch (VSC-KWT Series). To avoid residual contaminants from the CASS solution, the NSS test was carried out in a different salt spray chamber (Erichsen, Modell 608, 1000l). The Condensation test was performed in a climatic chamber from Ineltec (Model CKEST-300). The combined Thermal Cycling and Humidity test (TCH) was conducted in the Atlas weathering chamber SC340 and the UV and Humidity (UVH) test in the Atlas UVTest® using lamp type II (UVA-340) with a peak emission at 340 nm.

Prior and after each test, the reflectance of the samples was measured according to the actual SolarPACES reflectance measurement guideline [24]. The solar-weighted hemispherical reflectance, $\rho_{s,h}$, and the monochromatic near-specular reflectance, $\rho_{\lambda,\varphi}$, were determined. Nomenclature is based on [24] and [25].

The spectral hemispherical reflectance, $\rho_{\lambda,h}$, was measured in the wavelength range of λ = [280-2500] nm, using 5 nm intervals at an incidence angle of $\theta_i = 8°$ with a Perkin-Elmer Lambda 1050 spectrophotometer with an integrating sphere of 150 mm diameter [26]. The data was evaluated with a 2nd surface reference reflectance standard (calibrated in the range 280-2500 nm), traceable to NIST. Three measurements were taken on each sample, rotating the sample by 90º each time to detect possible anisotropies. Solar-weighted hemispherical reflectance $\rho_{s,h}$ was calculated following the weighting formula described in [27] using the direct normal Air Mass 1.5 ASTM G173-03 standard spectral irradiance distribution [28]. In a similar way, $\rho_{ISO,h}$ was determined, with the only difference that the spectral irradiance distribution defined in ISO 9050 [29] was used for the weighting.

The monochromatic near-specular reflectance $\rho_{\lambda,\varphi}$ within a defined acceptance half-angle of φ = 12.5 mrad, was measured with a Devices & Services 15R-USB portable specular reflectometer [26]. This instrument uses a parallel beam with an incidence angle of θ_i = 15° and a wavelength range between 635 and 685 nm, with a peak at λ = 660 nm. Each sample was measured in five different positions. The

acceptance angle selected is considered to be appropriate for parabolic-trough collectors of Eurotrough type.

In spite of its importance for CSP technology, the current commercial equipment to measure near-specular reflectance is limited to single wavelength instruments at near-normal incidence angles and acceptance angles $\varphi \geq 7.5$ mrad [30]. For heliostats in solar towers the relevant acceptance angles might be as low as $\varphi = 2$ mrad. To overcome the drawbacks of commercial measurement equipment, several research institutes are developing advanced characterization techniques and models to determine the solar-weighted near-specular reflectance [31], [32], [33], [34], [35], [36]. Since the developments are still not commercially available, the SolarPaces Reflectance guideline proposes to characterize the specular quality of the mirror, by comparing the monochromatic near-specular reflectance, $\rho_{\lambda,\varphi}$, with the monochromatic hemispherical reflectance, $\rho_{\lambda,h}$, at same wavelength and at near-normal incidence, which should show approximately the same value for a mirror without scattering effects. In this paper, this comparison has been carried out for $\lambda = 660$ nm and φ=12.5 mrad and the Specularity, $S_{\lambda,\varphi}$, is being introduced:

$$S_{\lambda,\varphi} = \frac{\rho_{\lambda,\varphi}}{\rho_{\lambda,h}} \quad (1)$$

For an ideal specular mirror $S_{\lambda,\varphi}$=1.

The repeatability of the reflectance measurements is 0.002 for both, the Perkin Elmer Lambda 1050 and the Devices & Services 15R-USB instruments. The absolute measurement uncertainty is 0.007, since the uncertainty related to the reference mirror traceable to NIST is 0.5%.

Finally, images of selected degradation spots were acquired with the 3D light microscope Axio CSM 700 by ZEISS or the SEM model S 3400N by Hitachi. Photographic analysis was performed using a Nikon D300S SLR camera. Maximum edge corrosion penetration was measured manually using a rule. Corrosion spot density in the silver layer was determined by counting with naked eye or in case of significant corrosion by an image analysis tool developed with Matlab®. The blistering level of the samples was determined according to the standard ISO 4628-2 [37].

3. Results and discussion

3.1 Initial reflectance (before aging)

3.1.1 Specularity of 4 mm silvered-glass mirrors

The reflectance parameters $\rho_{\lambda,h}$ and $\rho_{\lambda,\varphi}$ of commercially available 4 mm silvered-glass reflectors are plotted in Figure 3, in which (such as in the subsequent plots of this

paper) one data point corresponds to the average of the measurements taken on a single sample. A total of 62, 29, 61, 54, 22 and 17 samples have been evaluated for manufacturers A-F. The obtained average values are: $S_{\lambda,\varphi}$ = 0.997 ± 0.002; $\rho_{\lambda,h}$ = 0.958 ± 0.003 and $\rho_{\lambda,\varphi}$ = 0.956 ± 0.004.

In Figure 3 it can be seen that some mirror samples exhibit specularities above 1 ($S_{\lambda,\varphi}$ >1), which is physically not possible. This is caused by the uncertainty due to the measurement repeatability of the employed equipment. For that reason, mirrors with specularities in the range $S_{\lambda,\varphi}$ = [0.998, 1] can be considered as perfectly specular. Specularities in the range $S_{\lambda,\varphi}$ = [0.996, 0.998) can be considered as acceptable, while specularities in the range $S_{\lambda,\varphi}$ =[0, 0.996) are regarded as below the state of the art. Only 6.5% of the 245 measured mirrors exhibited $S_{\lambda,\varphi}$ below the state of the art.

As indicated by the gray box in Figure 3, mirrors with 0.996 ≤ $S_{\lambda,\varphi}$ ≤ 1; 0.955 ≤ $\rho_{\lambda,h}$ ≤ 0.962 and 0.953 ≤ $\rho_{\lambda,\varphi}$ ≤ 0.960 can be considered as the state of the art. All manufacturers were capable to produce samples with these characteristics although especially manufacturers B, C and F also produced samples below the state of the art. The high dispersion of samples from manufacturers A, B, C indicate differences in the manufacturing charges, while as production of manufacturers D, E, F seems to be more stable across the batches. At the other end, several mirrors from manufacturer A showed to exceed the state of the art reflectance characteristics.

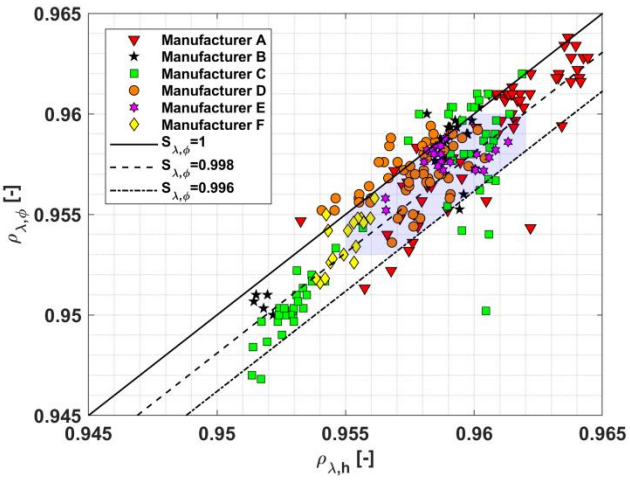

Figure 3: Monochromatic near-normal hemispherical and monochromatic near-specular reflectance at λ=660 nm of commercial 4 mm glass mirrors. The gray area can be considered as state of the art.

3.1.2 Solar-weighted hemispherical reflectance of 4 mm glass mirrors

The solar-weighted hemispherical reflectance $\rho_{s,h}$ and the corresponding specularity $S_{\lambda,\varphi}$ of the measured mirror samples are shown in Figure 4. Mirrors with 0.996 ≤ $S_{\lambda,\varphi}$ ≤ 1

and $0.941 \leq \rho_{s,h} \leq 0.948$ can be considered as the state of the art as indicated by the gray box. Again, all manufacturers manage to meet these characteristics but the variations in production charges clearly show that some samples exhibit worse properties. The highest solar-weighted reflectance achieved is $\rho_{s,h} > 0.95$ at perfect specularity by manufacturer A.

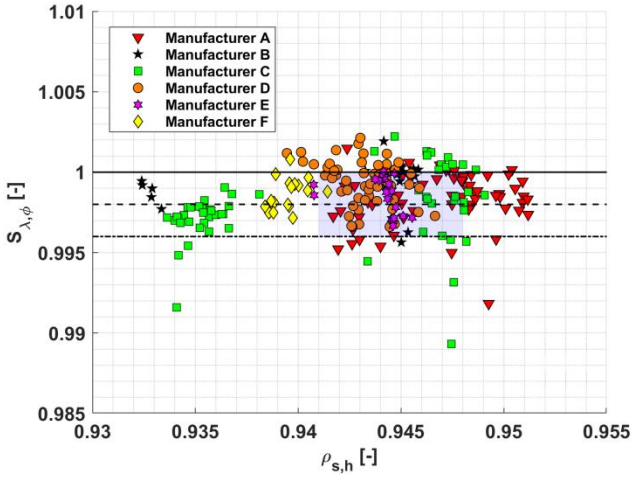

Figure 4: Solar-weighted hemispherical reflectance, $\rho_{s,h}$, plotted over specularity, $S_{\lambda,\varphi}$, of commercial 4 mm silvered-glass mirrors. The gray area can be considered as state of the art.

3.1.3 Influence of the reference spectrum for solar weighting of 4 mm glass mirrors

Figure 5 shows the difference in solar-weighted hemispherical reflectance results obtained when performing the solar-weighting with the ISO9050, $\rho_{ISO,h}$, and ASTM G173, $\rho_{s,h}$, solar reference spectra. It can be seen that $\rho_{ISO,h}$ shows a constant offset of around 0.0026 compared to $\rho_{s,h}$ in the range of interest. For this reason, when referring to $\rho_{ISO,h}$-values, the range of the state of the art can be resized to $0.938 \leq \rho_{ISO,h} \leq 0.945$.

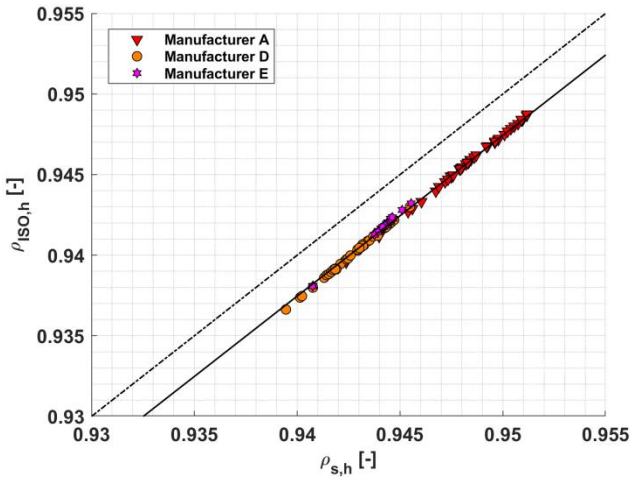

Figure 5: Hemispherical reflectance spectra weighted with ASTM and ISO reference spectra for 3 types of commercial 4 mm silvered-glass mirrors.

3.1.4 Influence of the glass thickness

In contrast to the expected behavior, the glass thickness of the available commercial mirrors shows a negligible effect on the measured average $\rho_{s,h}$. The curve shown in Figure 6 was obtained by averaging the measurements of samples from different silvered-glass mirror manufacturers from several manufacturing charges. The 1 and 3 mm data points were evaluated by averaging two different manufacturers respectively, the 2 mm data point by averaging three manufacturers, and the 4 mm data point by averaging six manufacturers. In total, 145, 387, 31 and 245 samples of 1, 2, 3 and 4 mm thickness respectively, were measured from 9 different manufacturers (some manufacturers provided samples with different glass thickness).

It can thus be concluded that the aforementioned state of the art requirements for 4 mm glass mirrors shall also be applicable to mirrors of lower thickness.

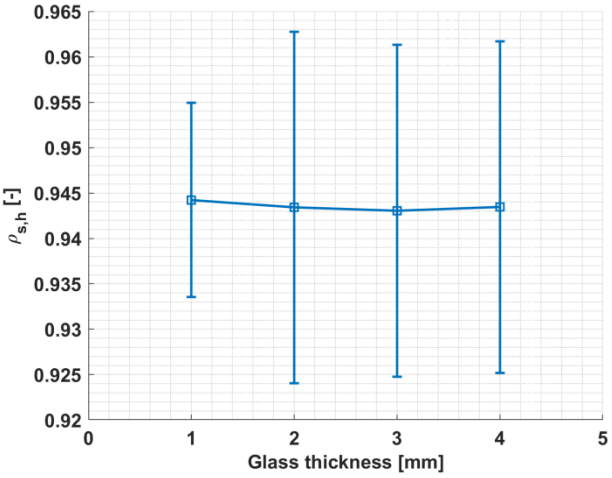

Figure 6: Influence of the glass thickness on solar-weighted hemispherical reflectance of commercially available solar reflectors

3.2 Reflectance loss during accelerated aging

In the following sections the measured reflectance loss during different accelerated aging tests is presented for six manufacturers of silvered-glass mirrors. The reflectance loss was computed by subtracting the reflectance after accelerated testing of each sample from its initial reflectance. The data is presented with a color scale, in which green color ($-0.002 \leq \Delta\rho \leq 0.002$) represents non-detectable losses (within the repeatability uncertainty of the measurement equipment); yellow ($0.002 < \Delta\rho \leq 0.004$) slight losses; orange ($0.004 < \Delta\rho \leq 0.007$) moderate losses; and red ($0.007 < \Delta\rho$) are considered high reflectance losses.

3.2.1 NSS Test

Figure 7a and Figure 8 show the measured hemispherical and near-specular reflectance losses during the NSS test for the different silvered-glass mirror manufacturers. As can be seen, monochromatic near-specular reflectance may reach moderate losses after the recommended testing time of 480 hours by UNE. The reflectance loss is greatly influenced by glass corrosion (see Figure 7b), while the silver layer shows no corrosion or tarnishing for almost all of the tested samples after 480 hours of testing. Glass corrosion is caused by the combination of high humidity at elevated temperature in the climatic chambers. Protecting the glass side with an adhesive tape is a recommended practice to prevent glass corrosion and to be able to differentiate silver corrosion processes and eventual glass corrosion processes, which is a phenomenon that has not been found in outdoor conditions. This becomes especially relevant for testing times beyond 480 hours. Consequently, it is

recommended to avoid the testing without a proper glass protection, especially in long-term tests.

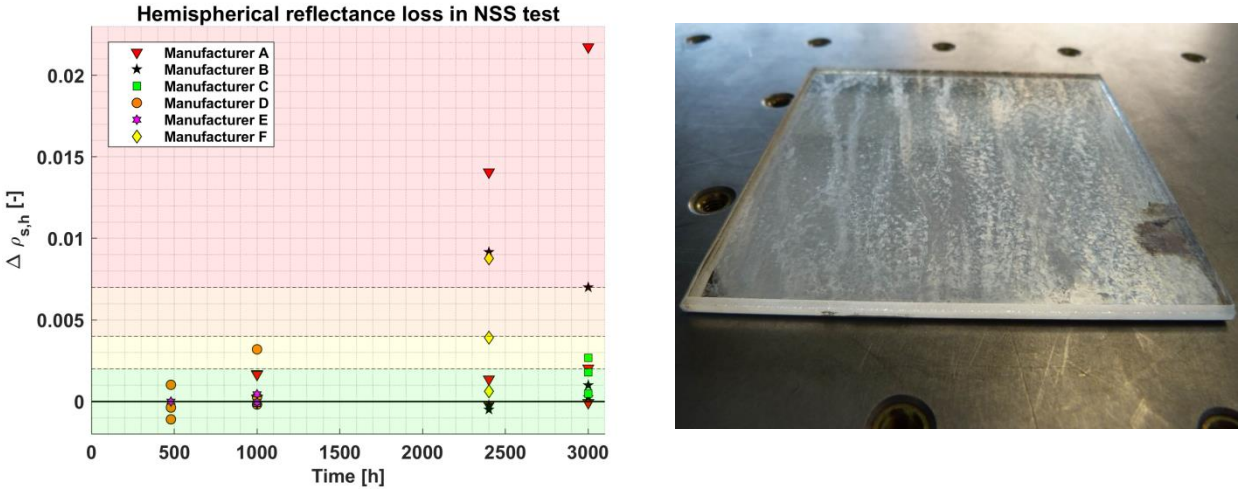

Figure 7 a): Hemispherical reflectance loss during NSS testing. b) Glass corrosion on 10x10 cm² silvered-glass mirror sample after 3000 hours of NSS testing

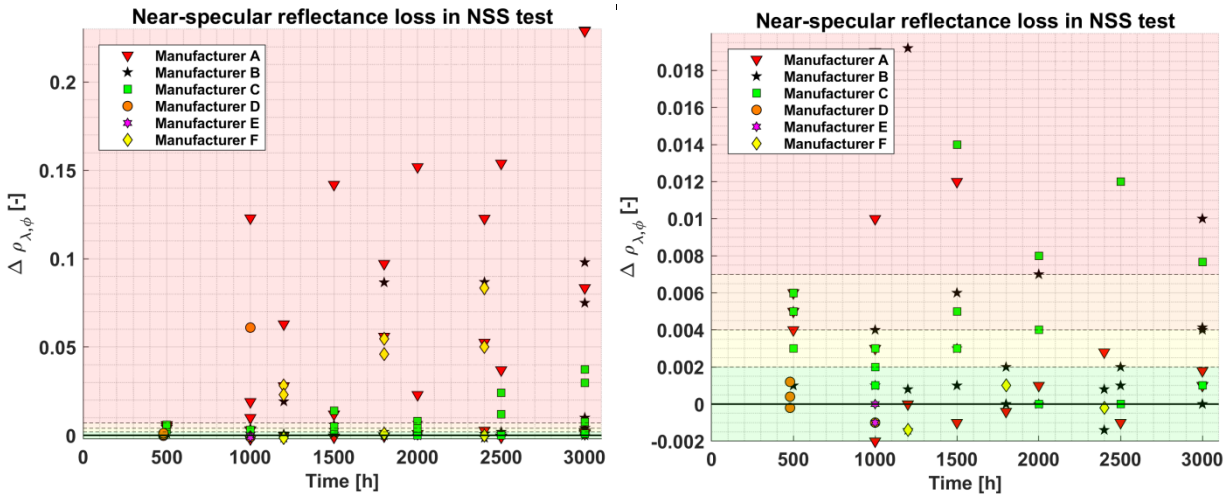

Figure 8 Near-specular reflectance loss during NSS testing a) Full data set. b) Reduced scale

3.2.2 CASS Test

The measured hemispherical and near-specular reflectance losses during CASS testing are shown in Figure 9 and Figure 10. For testing times >750 hours significant degradation is appreciated, mainly in specular reflectance. However, for the short term test of 120 hours proposed by UNE, non-detectable reflectance losses may be considered as state of the art.

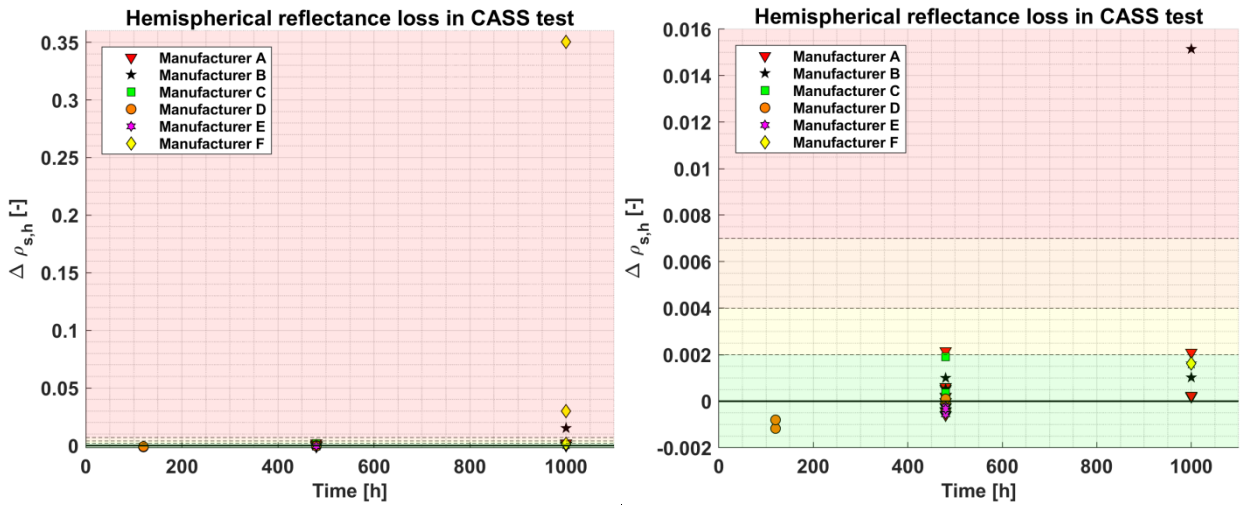

Figure 9 Hemispherical reflectance loss during CASS testing a) Full data set. b) Reduced scale

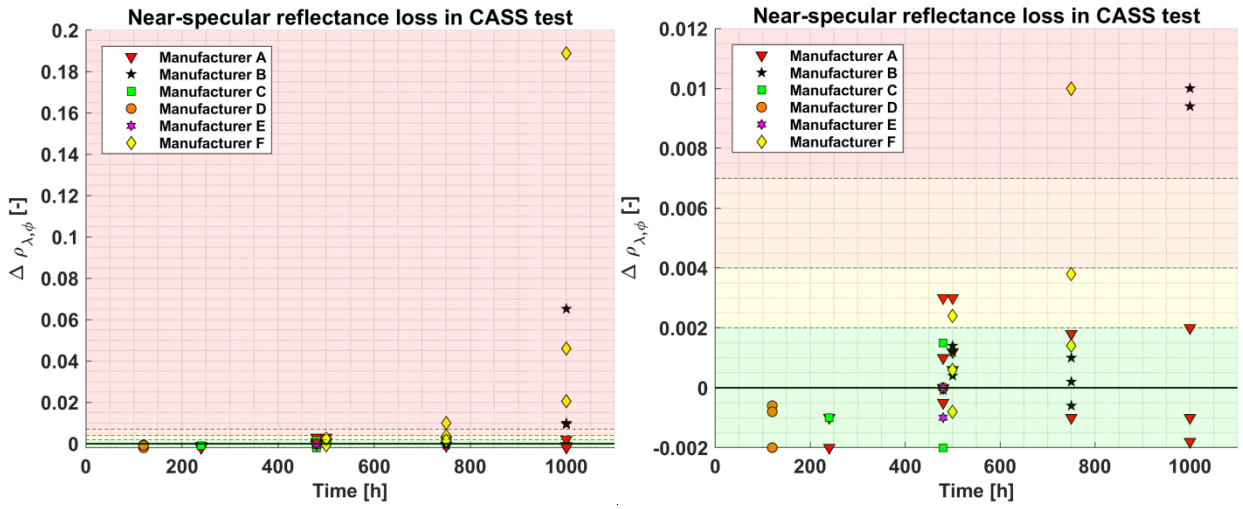

Figure 10 Near-specular reflectance loss during CASS testing a) Full data set. b) Reduced scale

3.2.3 Condensation Test

Figure 11 shows the measured reflectance losses during the Condensation test. This test has only been carried out for four of the six manufacturers. After the required 480 hours by UNE non-measurable reflectance losses can be considered as state of the art. Also, for longer testing time (up to 980 hours) non-measurable reflectance losses were found.

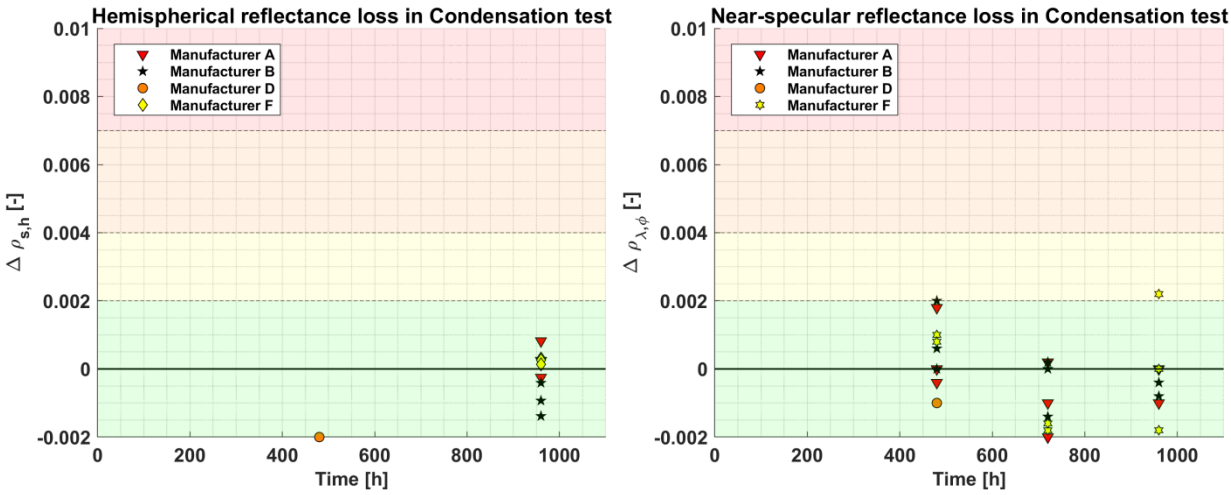

Figure 11 Reflectance loss during Condensation testing a) Hemispherical reflectance loss. b) Near-specular reflectance loss

3.2.4 Combined Thermal Cycling and Humidity (TCH)Test

The measured reflectance losses of the TCH test are shown in Figure 12. Three different options of TCH testing are defined in [14]. This test has only been carried out for four of the six manufacturers. Samples from manufacturer D have been tested according to Method A, while samples from manufacturer F have been tested according to method B2. In addition, samples from manufacturers A, D and E have been tested according to method B2 with the modification that the initial 4 hours of the cycle are performed at 65°C instead of 85°C. Only limited data is available for this test so far but the fact that all manufacturers reached non-detectable reflectance losses (even after 24 cycles of testing in the case of manufacturer F) permits to require non-detectable losses after 10 cycles as state of the art.

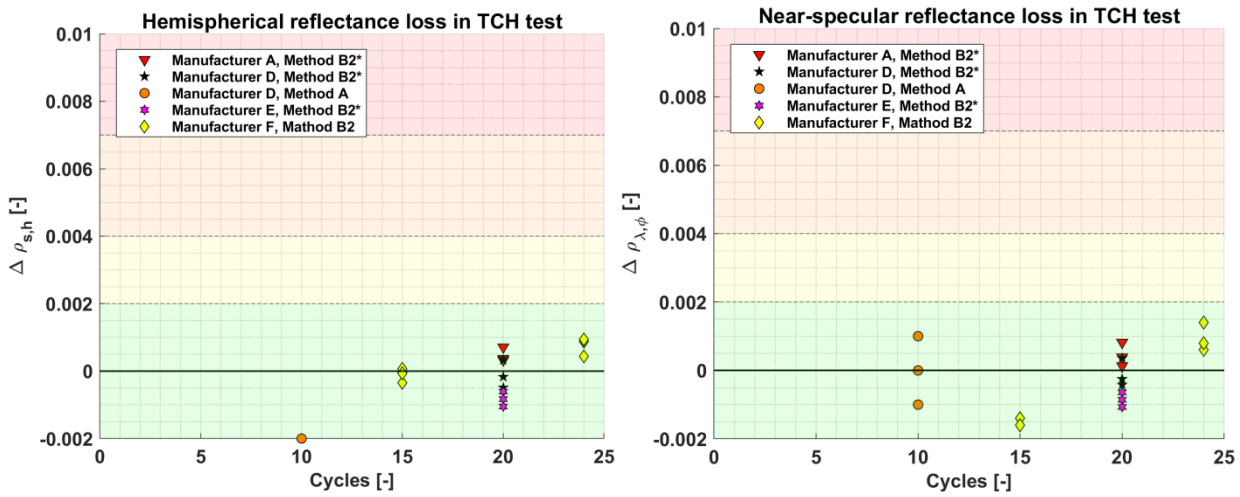

Figure 12 Reflectance loss during Thermal Cycling and Humidity testing a) Hemispherical reflectance loss. b) Near-specular reflectance loss

3.2.5 UV and Humidity Test

Figure 13 shows the measured reflectance losses during UVH testing. After the recommended 2000 hours by UNE, some samples from manufacturers A, B and C show moderate reflectance losses. At the same time, both manufacturers managed to produce samples with non-detectable losses after 2000 hours. Slight losses ($0.002 < \Delta\rho \leq 0.004$) after 2000 hours can be regarded as state of the art. In addition, only a few samples presented high reflectance losses ($0.007 < \Delta\rho$), after the maximum tested time of 3000 hours.

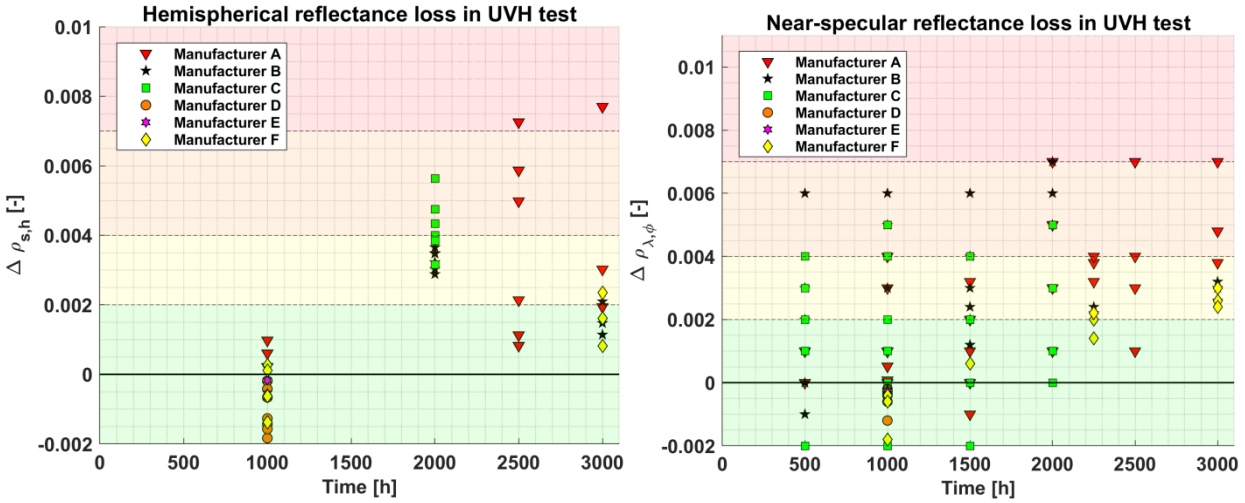

Figure 13 Reflectance loss during UV and Humidity testing a) Hemispherical reflectance loss. b) Near-specular reflectance loss

3.3 Edge corrosion penetration during accelerated aging

Figure 14 shows the appearing edge corrosion at the originally sealed edge during accelerated testing. The CASS test is the only test showing detectable edge corrosion, therefore no data is presented for the other accelerated tests. Also, data points for samples where no edge corrosion was detectable were omitted in the graph. It can be concluded that edge corrosion starts to show at testing times ≥480 hours. Hence, minimum edge corrosion ($l_{corr} \leq 0.1$ cm) should be required for the UNE tests.

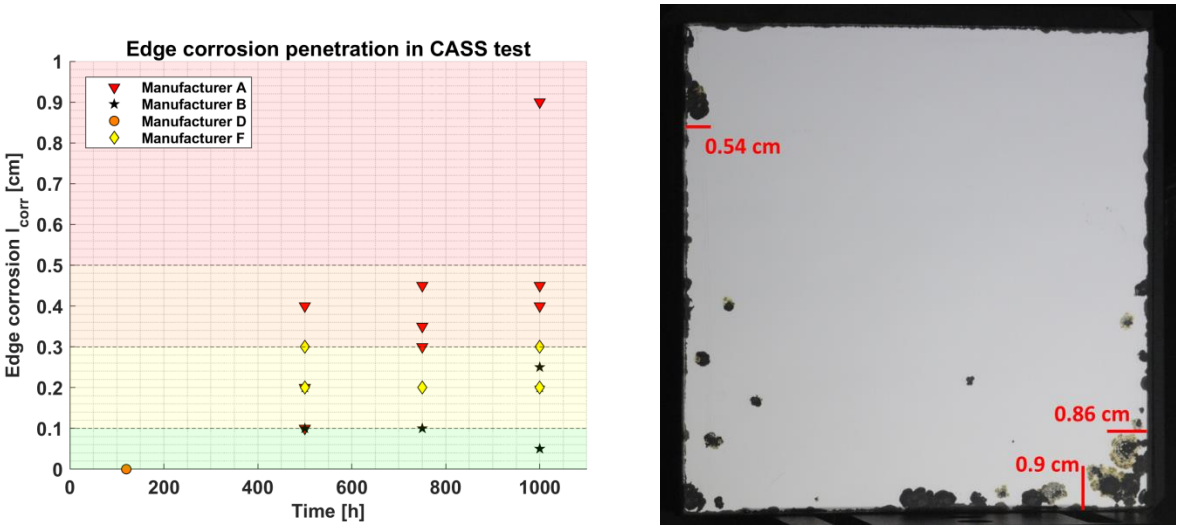

Figure 14 a) Maximum appearing penetration of corrosion starting from protected edge of the sample during the CASS test. b) Example of edge corrosion of 0.9 cm after 1000 hours of CASS testing on 10x10cm² sample with 4 sealed edges.

3.4 Localized spot corrosion during accelerated aging

The density of corrosion spots with diameter larger than 200 µm is shown in Figure 15. The data is grouped by accelerated aging tests and not by manufacturer like in the previous graphs. Data points for samples where no corrosion spots were detected, were omitted in the graph. In the CASS test, corrosion spots form the quickest. After 120 hours of testing, a maximum of 1 corrosion spot per 10 x 10 cm² sample can be considered as state of the art. The same limit may be applied for 480 hours of NSS and Condensation testing, as well as 10 cycles of TCH and 2000 hours of UVH testing.

No acceptance limit in corrosion spot size is defined. Large corrosion spots or a high number of small spots smaller than 200 µm will cause failure of the reflectance loss criterion.

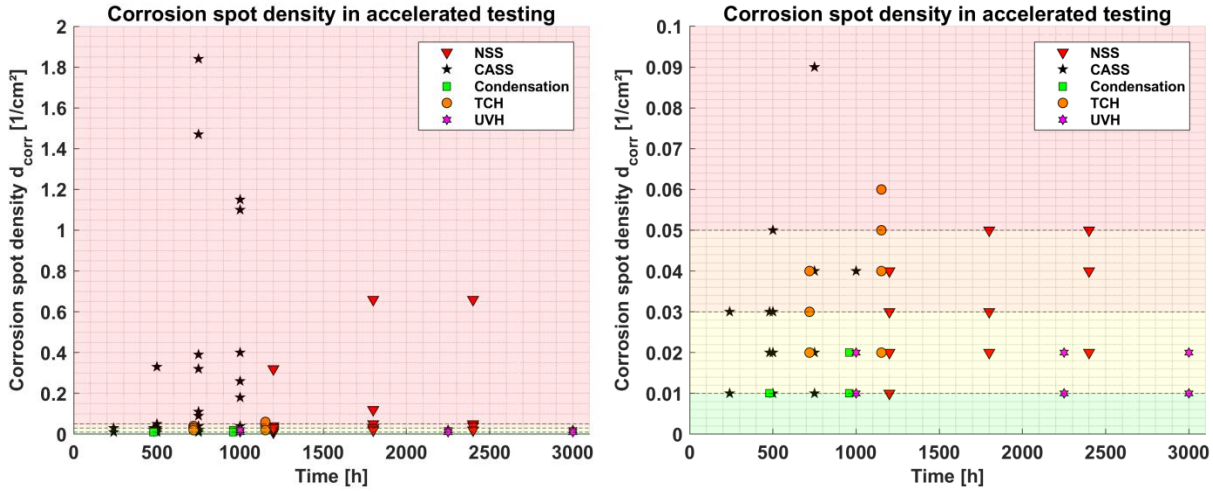

Figure 15 Spot density of corrosion spots >200 µm during different accelerated aging tests a) Full data set. b) Reduced scale

3.5 Blistering of protective paints during accelerated aging

Figure 16a shows the appearing blistering level in different accelerated aging tests according to the ISO 4628-2 standard [37]. The ISO standard characterizes the blistering level with two parameters: the blistering density (counted from 0 to 5, where 0 represents no blistering and 5 a high density) and the size of the blisters (counted from 1 to 5, where 1 represents microscopic size and 5 blisters larger than 5 mm in diameter). Examples of blistering in the protective paint layers are shown in Figure 16b and Figure 17. The testing times of 120 hours of CASS and 480 hours of NSS proposed by UNE should not cause any blistering on the tested samples, while as for 480h of Condensation, 10 cycles of TCH and 2000h of UVH a blistering level ≤1(≤S4) (the first number referring to blister density, the second one to blister size) shall be admissible.

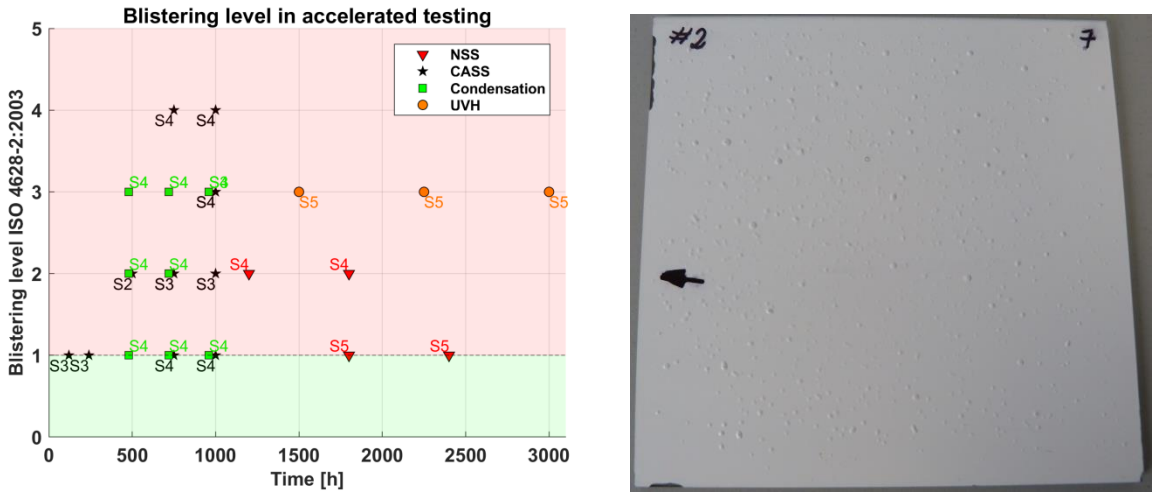

Figure 16 a) Blistering level in different accelerated aging tests according to ISO 4628-2:2003. The level on the y-axis represents the density of blisters (0: none – 5: high), the data labels represent the size of blisters (S1: none – S5: >5mm). b) Example of blistering level 4(S4) after 1000 hours of CASS testing on 10x10cm² sample

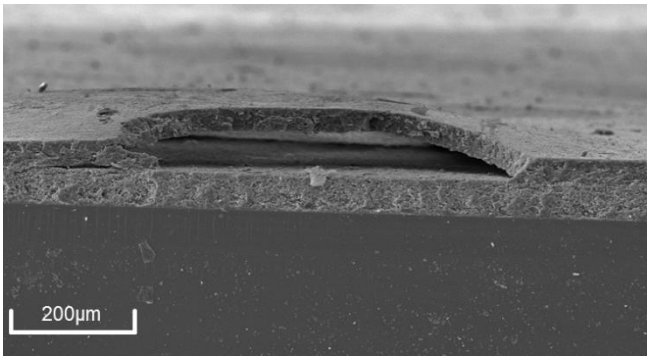

Figure 17 Cross section of S3 blister in protective paint layer after 240 hours of CASS testing.

3.6 Proposed acceptance criteria for mirror qualification according to UNE 206016:2018

The conclusions from the previous sections are summarized in Table 2 and Table 3. Table 2 provides guidance to benchmark initial reflective properties of mirror samples compared to what the authors consider as state of the art. As explained in 3.1.4, the defined criteria in Table 2 and Table 3 shall also be applicable to silvered-glass mirrors with deviant thickness of 4 mm.

Table 2: Proposed rating criteria to compare the reflectance characteristics of silvered-glass mirrors in their initial state (before aging)

Parameter	Symbol	Rating	
Solar-weighted hemispherical reflectance (weighted with ASTM G173 reference spectrum)	$\rho_{s,h}$	(0.948, 1] [0.941, 0.948] [0, 0.941)	exceeds state of the art state of the art below the state of the art
Solar-weighted hemispherical reflectance (weighted with ISO 9050 reference spectrum)	$\rho_{s,ISO}$	(0.945, 1] [0.938, 0.945] [0, 0.938)	exceeds state of the art state of the art below the state of the art
Hemispherical reflectance at 660nm	$\rho_{\lambda,h}$	(0.962, 1] [0.955, 0.962] [0, 0.955)	exceeds state of the art state of the art below the state of the art
Near-specular reflectance at 660nm and 12.5 mrad	$\rho_{\lambda,\varphi}$	(0.960, 1] [0.953, 0.960] [0, 0.953)	exceeds state of the art state of the art below the state of the art
Specularity at 660 nm and 12.5 mrad	$S_{\lambda,\varphi}$	[0.996, 1] [0, 0.996)	state of the art below the state of the art

Table 3 shows the proposed acceptance criteria for the accelerated aging tests of the UNE standard. As explained in 3.2.1, for samples suffering from glass corrosion, application of a protective adhesive tape on the glass side may be used on all tested samples to reach the reflectance goals.

Table 3 Proposed acceptance criteria for silvered-glass mirror testing according to the minimum testing time proposed in UNE 206016:2018

	Admissible $\Delta\rho_{s,h}$	Admissible $\Delta\rho_{\lambda,\varphi}$	Admissible l_{corr}	Admissible d_{corr}	Admissible blistering level [37]
NSS, 480h	Slight (≤0.004)	Slight (≤0.004)	≤ 0.1 cm	≤ 0.01 cm^{-2}	0(S1)
CASS, 120h	None (≤0.002)	None (≤0.002)	≤ 0.1 cm	≤ 0.01 cm^{-2}	0(S1)
Condensation, 480h	None (≤0.002)	None (≤0.002)	≤ 0.1 cm	≤ 0.01 cm^{-2}	≤1(≤S4)
TCH, 10 cycles	None (≤0.002)	None (≤0.002)	≤ 0.1 cm	≤ 0.01 cm^{-2}	≤1(≤S4)
UVH, 2000h	Slight (≤0.004)	Slight (≤0.004)	≤ 0.1 cm	≤ 0.01 cm^{-2}	≤1(≤S4)

3.7 *Correlation of accelerated aging testing to outdoor exposure*

The corroded area fraction, A_{corr}, has been monitored during CASS testing and compared to outdoor exposed samples (see Figure 18). After approximately 1000 hours a similar level of corrosion compared to three year outdoor exposure at a site of corrosivity CX (extreme corrosivity according to ISO 9223 [38]) in the Middle East is

reached. As rough estimation, one can deduce an acceleration factor of $a \approx 26$, meaning that 120 hours of CASS test would approximately simulate 4.3 months of exposure in a CX environment. Corrosivity classes of desert sites are usually much lower, in the range of C2/C3. Unfortunately, not enough corrosion data from desert sites are available to derive a meaningful correlation for low-corrosivity sites. Further research is required also to derive reliable correlations for other accelerated aging tests such as NSS, Condensation, THC and UVH.

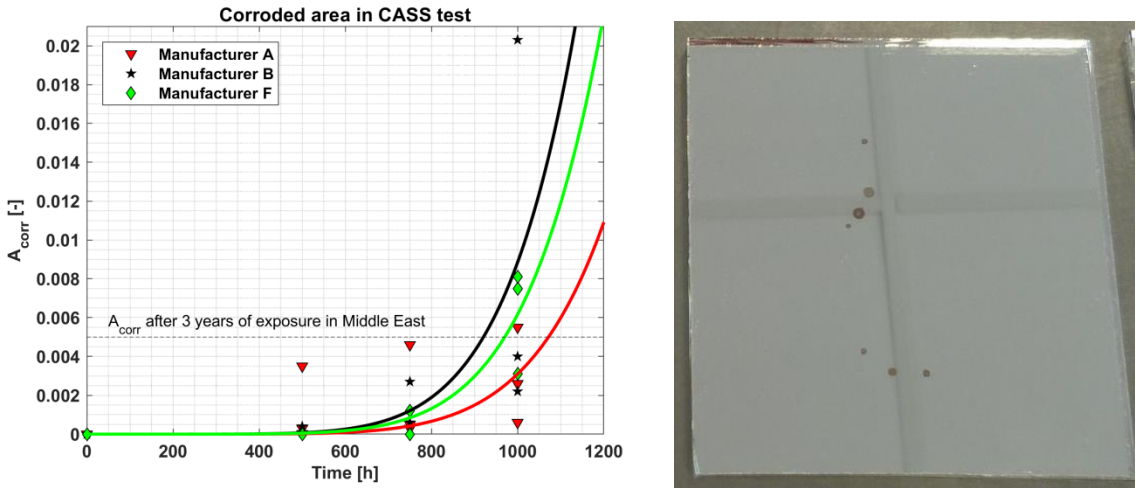

Figure 18 a) Corroded area fraction A_{corr} of three silvered-glass mirror types during CASS test compared to outdoor exposed samples of manufacturer C. b) Silvered-glass mirror from manufacturer C after 3 years of exposure in extremely corrosive site in the Middle East

4. Conclusion

This paper developed acceptance criteria for mirror qualification according to the new CSP reflector standard UNE 206016:2018, which lacks of such acceptance criteria up to date. To this end, a large dataset of reflectance measurements, collected over the past 5 years from all commercial silvered-glass mirror manufacturers, was presented. Analysis of the data permitted to define that solar-weighted reflectance in the range of [0.941, 0.948] with specularitiy of [0.996, 1] can be considered as state of the art.

Accelerated aging tests were carried out far beyond the required testing times in the UNE standard, which served as basis to define acceptance criteria for conditions defined by UNE and to acquire useful information about the behavior of the mirrors in long-term testing. The new acceptance criteria will extend to the scope of the standard, permitting to rate the obtained degradation results and benchmark them against the current state of the art. Non-detectable / slight reflectance losses up to 0.004 shall be admissible for the accelerated aging tests defined by UNE. The UNE tests can thus be

regarded as a method to check if a mirror fulfills the minimum requirements for outdoor application. However, more aggressive accelerated aging programs are useful to conduct comparative testing since more severe degradation on the specimens is required to carry out a meaningful material comparison.

Correlating the UNE test results to an actual life-span in different outdoor environments is not possible by the current state of the art. More degradation data from outdoor exposed mirror samples is required for this purpose. However, as first estimate an acceleration factor of 26 was derived for the CASS test with respect to an outdoor exposure site of extreme corrosivity.

5. Nomenclature

CASS	Copper accelerated salt spray test according to ISO9227
CIEMAT	*Centro de Investigaciones Energéticas Medioambientales y Tecnológicas* (Energy, Environment and Technology Research Centre, Spain)
CSP	Concentrated Solar Power
DLR	*Deutsches Zentrum für Luft- und Raumfahrt* (German Aerospace Centre, Germany)
NSS	Neutral salt spray test according to ISO9227
OPAC	Optical Aging Characterization laboratory at *Plataforma Solar de Almería*, Spain
SEGS	Solar Energy Generating Systems in Mojave Desert, California
SEM	Scanning electron microscope
TCH	Thermal Cycling and Humidity test according to UNE 206016:2018, Method A / Method B2
UNE	Spanish Association for Standardization
UVH	UV and Humidity test according to ISO 16474-3

a	acceleration factor [-]
A_{corr}	corroded area fraction [-]
d_{corr}	corrosion spot density [1/cm²]
l_{corr}	maximum penetration of corrosion starting from edge of sample [cm]
$S_{\lambda,\varphi}$	Specularity at λ= 660 nm, φ= 12.5 mrad
θ_i	incidence angle in °
λ	wavelength in nm
$\rho_{ISO,h}$	solar-weighted hemispherical reflectance in the range λ =[280-2500]nm at θ_i = 8°. The weighting is performed with the direct normal Air Mass 1.5 reference spectrum specified in ISO 9050.
$\rho_{s,h}$	solar-weighted hemispherical reflectance in the range λ =[280-2500]nm at θ_i = 8°. The weighting is performed with the direct normal Air Mass 1.5 ASTM G173 reference spectrum.
$\rho_{\lambda,h}$	spectral hemispherical reflectance at wavelength λ. For the measurements in this paper: θ_i = 8°, λ = 660 nm.

$\rho_{\lambda,\varphi}$ near-specular reflectance at wavelength λ, incidence angle θ_i and acceptance angle φ. For the measurements in this paper: θ_i = 15°, λ = 660 nm, φ = 12.5 mrad

φ acceptance half-angle in mrad related to the mirror scattering. Here φ = 12.5 mrad.

6. Acknowledgements

This project has received funding from the European Union's Horizon 2020 research and innovation program under grant agreement No 686008, project RAISELIFE.
Moreover, the authors would like to thank the Moroccan research institute IRESEN for the collaboration on mirror exposure in Moroccan climate and meteorological data analysis.

7. Literature

[1] Kennedy, C.: Advances in Reflector and Solar Selective Materials for Application to Concentrating Solar Power Systems, CIMTEC 2010, 5th Forum on new materials, Montecatini Terme, Italy

[2] Sutter, F.; Ziegler, S.; Schücker, M.; Heller, P.; Pitz-Paal, R.: Modelling of optical durability of enhanced aluminum solar reflectors. Sol. Energy Mater. Sol. Cells. 107, 37-45. 2012

[3] Kennedy, C.; Terwilliger, K.: Optical Durability of Candidate Solar Reflectors. J. Sol. Energy Eng. 127, 262-269. 2005

[4] Wiesinger, F.; Sutter, F.; Wolfertstetter, F.; Hanrieder, N.; Fernández-García, A.; Pitz-Paal, R.; Schmücker, M.: Assessment of the erosion risk of sandstorms on solar energy technology at two sites in Morocco. Sol. Energy 162, 2017-228. 2018

[5] García-Segura, A.; Fernández-García, A.; Ariza, M.J.; Sutter, F.; Valenzuela, L.: Degradation of concentrating solar thermal reflectors in acid rain atmospheres. Solar Energy Materials and Solar Cells. 186, 92-2014. 2018

[6] Sutter, F.; Fernandez, A.; Heller, P.; Anderson, K.; Wilson, G.; Schmücker, M.; Marvig, P.: Durability testing of silvered-glass mirrors, Energy Procedia 69, 1568 – 1577. 2015

[7] García-Segura, A.; Fernández-García, A.; Ariza, M.J.; Valenzuela, L.; Sutter, F.: Durability studies of solar reflectors: A review. Renewable and Sustainable Energy Reviews, 62, 453-467. Doi: 10.1016/j.rser.2016.04.060. 2016

[8] Avenel, C.; Raccurt, O.; Gardette, J.; Therias, S.: Review of accelerated ageing test modelling and its application to solar mirrors, Solar Energy Materials and Solar Cells 186 (2018), 29-41. 2018

[9] Sutter, F.; Fernández-García, A.; Wette, J.; Wiesinger, F.: Assessment of durability and accelerated aging methodology of solar reflectors, in: Heller, P. (ed.), The

Performance of Concentrated Solar Power (CSP) Systems. Analysis, Measurement and Assessment. Elsevier, pp. 169-201. 2017

[10] Sutter, F.; Wette, J.; Fernández-García, A.; Ziegler, S.; Dasbach, R.: Accelerated aging testing of aluminum reflectors for concentrated solar power, SolarPaces guideline, 2016, available online under: http://www.solarpaces.org/tasks/task-iii-solar-technology-and-advanced-applications. Last access: 31st of August 2018.

[11] Wette, J.; Sutter, F.; Fernández-García, A.; Ziegler, S.; Dasbach, R.: Comparison of Degradation on Aluminum Reflectors for Solar Collectors due to Outdoor Exposure and Accelerated Aging. Energies. 9(916). 2016

[12] Sutter, F.; Wette, J.; Wiesinger, F.; Fernández-García, A.; Ziegler, S.; Dasbach, R.: Lifetime prediction of aluminum solar mirrors by correlating accelerated aging and outdoor exposure experiments, Solar Energy 174, 149-163. 2018

[13] Sallaberry, F.; Bello, A.; Burgaleta, J.I.; Fernandez-García, A.; Fernandez-Reche, J.; Gomez, J.A.; Herrero, S.; Lüpfert, E.; Morillo, R.; San Vicente G.; Sanchez, M.; Santamaria, P.; Ubach, J.; Terradillos, J.; Valenzuela, L.: Standards for components in concentrating solar thermal power plants - status of the Spanish working group. 21th SolarPACES 2015. International Conference on Concentrating Solar Power and Chemical Energy Systems. Cape Town (South Africa). October, 13-16. 2015

[14] UNE 206016:2018. Paneles reflectantes para tecnologías de concentración solar. 2018

[15] Sutter, F.; Fernández-García, A.; Wette, J.; Heller, P.: Comparison and evaluation of accelerated aging tests for reflectors. Energy Procedia. 49, 1718-1727. 2014

[16] ISO 9227:2017. Corrosion tests in artificial atmospheres - Salt spray tests. 2017

[17] ISO 6270-2:2017 Paints and varnishes - Determination of resistance to humidity - Part 2: Condensation (in-cabinet exposure with heated water reservoir). 2017

[18] ISO 16474-3:2014. Paints and varnishes – Methods of exposure to laboratory light sources - Part 3: Fluorescent UV lamps. 2014

[19] Sutter, F.; Wiesinger, F.; King, P.; Pagano, F. Bayon, R.; Imbuluzqueta, G.; Pescheux, A.: Report on the methodology of accelerated erosion testing for reflectors and absorbers, STAGE-STE project, https://www.stage-ste.eu/deliverables/STAGE_STE_Deliverable_8.5.pdf Last access: 31st of August 2018.

[20] Wiesinger, F.; Sutter, F.; Fernández-García, A.; Reinhold, J.; Pitz-Paal, R.: Sand erosion on solar reflectors: Accelerated simulation and comparison with field data. Solar Energy Materials and Solar Cells. 145 (2016), 303-313. 2016

[21] IEC 61215-2:2016 Terrestrial photovoltaic (PV) modules – Design qualification and type approval. Part 2: Test procedures. 2016

[22] IEC 62108:2007 Concentrator photovoltaic (cpv) modules and assemblies - designed modification and type approval. International electrochemical commission. 2007
[23] Wette, J.; Sutter, F.; Fernández-García, A.; Lahlou, R.; Armstrong, P.: Standardizing accelerated aging testing conditions for silvered-glass reflectors, Proceedings of the SolarPaces conference 2017, Santiago de Chile. 2017
[24] SolarPACES Reflectance Guideline: Parameters and Method to Evaluate the Reflectance Properties of Reflector Materials for Concentrating Solar Power Technology Technology. Version 3.0. March 2018. http://www.solarpaces.org/wp-content/uploads/20180320_SolarPACES-Reflectance-Guidelines-V3.pdf Last access: 31st of August 2018.
[25] UNE 206009:2013. Solar Thermal Electric Plants. Terminology. 2013
[26] Fernández-García, A.; Sutter, F.; Martínez-Arcos, L.; Sansom, C.; Wolfertstetter, F.; Delord, C.: Equipment and methods for measuring reflectance of concentrating solar reflector materials. Solar Energy Materials and Solar Cells, 167, 28-52. Doi: 10.1016/j.solmat.2017.03.036. 2017
[27] ASTM E903-82:2012: Standard Test Method for Solar Absorptance, Reflectance, and Transmittance of Materials Using Integrating Spheres, ASTM International. 2012
[28] ASTM G173-03:2003. Standard Tables for Reference Solar Spectral Irradiances: Direct Normal and Hemispherical on 37° Tilted Surface. 2003
[29] ISO 9050:2003 Glass in building - Determination of light transmittance, solar direct transmittance, total solar energy transmittance, ultraviolet transmittance and related glazing factors. 2003
[30] Sutter, F.; Montecchi, M.; von Dahlen, H.; Fernández-García, A.; Röger, M.: The effect of incidence angle on the reflectance of solar mirrors. Solar Energy Materials and Solar Cells 176 (2018) 119-133. 2018
[31] Montecchi, M.: Proposal of a New Parameter for the Comprehensive Qualification of Solar Mirrors for CSP Applications. AIP Conference Proceedings 1734, 130014; doi: 10.1063/1.4949224. 2016
[32] Sutter, F.; Meyen, S.; Fernandez-García, A.; Heller, P.: Spectral characterization of specular reflectance of solar mirrors. Solar Energy Materials and Solar Cells 145 (2016) 248-254. 2016
[33] Montecchi, M.: Approximated method for modelling hemispherical reflectance and evaluating near-specular reflectance of CSP mirrors, Solar Energy 92 (2013) 280-287. 2013
[34] Heimsath, A.; Schmid, T.; Nitz, P.: Angle resolved specular reflectance measured with VLABS. Energy Procedia 69 (2015) 1895 – 1903. 2015

[35] Meyen, S.; Sutter, F.; Heller, P.; Oschepkov, A.: A New Instrument For Measuring The Reflectance Distribution Function Of Solar Reflector Materials, Energy Procedia 49 (2014) 2145-2153. 2014
[36] Sutter, F.; Meyen, S.; Heller, P.; Pitz-Paal, R.: Development of a spatially resolved reflectometer to monitor corrosion of solar reflectors. Optical Mater. 35, 1600-1608. 2013
[37] ISO 4628-2:2003: Paints and varnishes, Evaluation of degradation of coatings - Designation of quantity and size of defects, and of intensity of uniform changes in appearance, Part 2: Assessment of degree of blistering. 2003
[38] ISO 9223:2012: Corrosion of metals and alloys - Corrosivity of atmospheres - Classification, determination and estimation. 2012